

A Computational Model of Monkey Grating Cells for Oriented Repetitive Alternating Patterns

T. Lourens, K. Nakadai, H.G. Okuno, and H. Kitano

Japan Science and Technology Corporation
ERATO, Kitano Symbiotic Systems Project
M. 31 Suite 6A, 6-31-15 Jingumae, Shibuya-ku, Tokyo 150-0001, Japan
{*tino, nakadai, okuno, kitano*}@symbio.jst.go.jp

Abstract. In 1992 neurophysiologists [5] found an new type of cells in areas V1 and V2 of the monkey primary visual cortex, which they called grating cells. These cells respond vigorously to a grating pattern of appropriate orientation and periodicity. A few years later a computational model inspired by these findings was published [3]. The study of this paper is to model a grating cell operator that responds in a very similar way as these grating cells do. Three different databases containing a total of 338 real world images of textures were applied to the operator. Based on these images, our findings were that grating cells respond best to repetitive alternating patterns of a specific orientation. These patterns are mostly human made structures, like buildings, fabrics, and tiles.

1 Introduction

Almost a decade ago, von der Heydt et al. [4, 5] reported on the discovery of a new type of neuron in areas V1 and V2 of the monkey visual cortex, they called them *grating cells*, because of their strong responses to grating patterns, but weakly to bars and edges. They estimated that these cells makeup around 4 and 1.6 percent of the population of cells in V1 and V2, respectively. The cells preferred spatial frequencies between 2.6 and 19 cycles per degree with tuning widths at half-amplitude between 0.4 and 1.4 octaves. They found that the cells are highly orientation selective and that the response is dependent on the number of cycles. A minimum of 2-6 cycles is required to evoke a response and leveled off at 4-14 cycles (median 7.5).

In this study we propose a computational model for these grating cells that meet the response profiles of the grating cells measured by von der Heydt et al. [5].

The paper is organized as follows: in Section 2 computational models of simple and complex cells are briefly introduced. These models are known from the literature, but since they form part of the grating cells they are included for completeness and clarity. A computational model of grating cells is given in Section 3. Also in this section the results of this model is compared with

measured responses of grating cells and an existing model for grating cells. Section 4 elaborates on the results of the model compared to the measured responses by applying the model to the same test patterns used by von der Heydt et al. In the same section the results of this model are compared with an existing model for grating cells. In Section 5 we apply the model to three databases to get better insights in the response of grating cells to real world images. The last section gives the conclusions.

2 Simple and complex cell operators

The receptive field profiles of simple cells can be modeled by complex-valued Gabor functions:

$$\hat{G}_{\sigma,\lambda,\theta}(x,y) = \exp\left(i\frac{\pi x_1}{\sqrt{2}\sigma\lambda}\right) \exp\left(-\frac{x_1^2 + \gamma^2 y_1^2}{2\sigma^2}\right), \quad (1)$$

where $x_1 = x \cos \theta + y \sin \theta$ and $y_1 = y \cos \theta - x \sin \theta$. Parameters σ , θ , λ , and γ represent scale, orientation, wavelength ($\frac{2}{\sqrt{2}\sigma\lambda}$ is the spatial frequency), and spatial aspect ratio, respectively. These Gabor functions have been modified such that their integral vanishes and their one-norm (the integral over the absolute value) becomes independent of σ , resulting in $G_{\sigma,\lambda,\theta}(x,y)$, for details see [2]. They provide a transform of the image $I(x,y)$ via spatial convolution. Afterwards, only the amplitudes of the complex values are retained for further processing:

$$C_{\sigma,\lambda,\theta} = \|I * G_{\sigma,\lambda,\theta}\|, \quad (2)$$

which represents our model for complex cell responses. Orientations and scales are sampled by $\theta_i = \frac{i \cdot 180}{N}$ and $\sigma_j = \sigma_{j-2} + \sigma_{j-1}$, where $i = 0 \dots N - 1$, $j = 2 \dots S - 1$, and σ_0 and σ_1 are known constants.

3 Grating cells

Von der Heydt et al. [4] proposed a model of grating cells in which the activities of displaced semi-linear units of the simple cell type are combined by a minimum operator to produce grating cell responses. This model responds properly to gratings of appropriate orientation and to single bars and edges. However, the model does not account for correct spatial frequency tuning.

Petkov and Kruizinga [3] proposed a model based on simple cell (with symmetrical receptive fields) input. Responses of simple cells are evaluated along a line segment by a maximum operator, then a quantity q is used to compensate for contrast differences. After that a point spread function is used to meet the spatial summing properties with respect to the number of bars and length. Except for the responses to the number of bars, this model does not meet the criteria for the grating cells measured by von der Heydt et al. One of the weak-points in this model is that it responds to other frequencies than the preferred frequency.

We propose a grating cell operator that meets the response profiles of the grating cells. This operator uses complex cell input responses, modeled by the operator given in (2). Likewise as in the other models, we evaluate the responses along a line segment perpendicular to the length of the bars of a grating. Unlike

the other models, we let the length depend on the similarity of the responses of the complex cells. No contrast normalization mechanism is incorporated in the grating operator, since we believe that this is compensated for at the stage of the center-surround cells already, see, e.g., Kaplan and Shapley [1].

3.1 Grating cell operator

The initial grating response is calculated as follows:

$$\mathbf{G}_{\sigma,\lambda,\theta,l}^{\text{avg}}(x,y) = \frac{\rho}{2l+1} \sum_{i=-l}^l \mathcal{C}_{\sigma,\lambda,\theta}(x+x_i, y+y_i), \quad (3)$$

where ρ is a response decrease factor. This factor is a measure for the deviation from the optimal frequency and uniformity of the complex cell responses, and will be discussed below. Parameter l denotes the length over which summation of the complex cell responses will take place.

The variable length $2l$ over which the responses of the complex cells will be evaluated is between the minimum number of bars $2B_{\min}$ and maximum number of bars $2B_{\max}$. Since the operations are performed on a discrete grid we decompose the maximum length from the center of the line segment, in x- and y-direction:

$$l_x = \frac{B_{\max}\sqrt{2}\sigma \cos \theta}{\lambda} \quad \text{and} \quad l_y = \frac{B_{\max}\sqrt{2}\sigma \sin \theta}{\lambda}. \quad (4)$$

Similarly, we decompose the minimum length (B_{\min}) into m_x and m_y . The preferred barwidth (in pixels) equals $\sigma\sqrt{2}\lambda$.

Depending on the preferred orientation θ , the evaluation will take place in x- or y-direction. Hence, parameters x_i , y_i , and l_{\max} of (3) are orientation dependent:

$$\begin{aligned} &\text{if } \left| \frac{l_y}{l_x} \right| \leq 1 \text{ and } l_x \neq 0 \\ &\quad x_i = i; \quad y_i = \lfloor i \frac{l_y}{l_x} + 0.5 \rfloor; \quad l_{\max} = \lfloor \lfloor l_x + 0.5 \rfloor \rfloor; \quad l_{\min} = \lfloor \lfloor m_x + 0.5 \rfloor \rfloor \\ &\text{else} \\ &\quad x_i = \lfloor i \frac{l_x}{l_y} + 0.5 \rfloor; \quad y_i = i; \quad l_{\max} = \lfloor \lfloor l_y + 0.5 \rfloor \rfloor; \quad l_{\min} = \lfloor \lfloor m_y + 0.5 \rfloor \rfloor \end{aligned} \quad (5)$$

where $\lfloor x \rfloor$ denotes the nearest integer value smaller than or equal to x . Length l of (3) is determined by the maximum, minimum, and average response of the complex cells along the line:

$$\begin{aligned} &l = \min_i(l_i), \quad l_{\min} < i \leq l_{\max}, \quad i \in \mathbb{Z} \quad \text{and} \\ &\text{if } \frac{\mathbf{G}_{\sigma,\lambda,\gamma,\theta,i}^{\max}(x,y) - \mathbf{G}_{\sigma,\lambda,\gamma,\theta,i}^{\text{avg}}(x,y)}{\mathbf{G}_{\sigma,\lambda,\gamma,\theta,i}^{\text{avg}}(x,y)} \geq \Delta \quad \text{or} \quad \frac{\mathbf{G}_{\sigma,\lambda,\gamma,\theta,i}^{\text{avg}}(x,y) - \mathbf{G}_{\sigma,\lambda,\gamma,\theta,i}^{\min}(x,y)}{\mathbf{G}_{\sigma,\lambda,\gamma,\theta,i}^{\text{avg}}(x,y)} \geq \Delta \\ &\quad l_i = i - 1 \quad \text{else} \quad l_i = l_{\max} \end{aligned} \quad (6)$$

Constant Δ , which is a uniformity measure, is a value larger than, but near 0. We used $\Delta = 0.25$ in all our experiments. The maximum and minimum \mathbf{G} responses are obtained as follows

$$\mathbf{G}_{\sigma,\lambda,\gamma,\theta,l}^{\Omega}(x,y) = \Omega_{i=-l}^l (\mathcal{C}_{\sigma,\lambda,\gamma,\theta}(x+x_i, y+y_i)) \quad , \quad (7)$$

where Ω denotes the min or max operator.

The determination of length l depends on the uniformity of responses of the complex cells along a line perpendicular to orientation θ . If the responses of these cells are not uniform enough the summation will be shorter than l_{\max} , and consequently the responses will be less strong. We model a linearly increasing response between B_{\min} and B_{\max} :

$$\rho_l = \frac{\frac{l}{l_{\max}}B_{\max} - B_{\min}}{B_{\max} - B_{\min}} = \frac{l - l_{\min}}{l_{\max} - l_{\min}}. \quad (8)$$

The modeled response also depends on the uniformity of the complex cell responses. Since ρ_l gives a strong decrease for short lengths (it equals 0 for l_{\min}), we do not decrease the response for length between the minimum number of bars and the minimum number plus one:

$$\text{if } (l_s \leq l_{\min}) \quad \rho_u = 1 \quad \text{else} \quad \rho_u = 1 - \frac{\mathbf{G}_{\sigma,\lambda,\gamma,\theta,l_s}^{\max}(x,y) - \mathbf{G}_{\sigma,\lambda,\gamma,\theta,l_s}^{\min}(x,y)}{2\Delta\mathbf{G}_{\sigma,\lambda,\gamma,\theta,l_s}^{\text{avg}}(x,y)} \quad (9)$$

where $l_s = l - \frac{l_{\max}}{1 + \lfloor B_{\max} \rfloor}$ is the length that is one bar shorter in length than l . The evaluation on a slightly shorter length ensures that both criteria in (6) are less than Δ , which implies that $\rho_u \geq 0$. Multiplying factors ρ_l and ρ_u results in the response decrease factor $\rho = \rho_l\rho_u$ from (3).

A weighted summation is made to model the spatial summation properties of grating cells with respect to the number of bars and their length and results in the grating cell responses at a single scale and orientation:

$$\mathcal{G}_{\sigma,\lambda,\theta,\beta} = \mathbf{G}_{\sigma,\lambda,\theta,l}^{\text{avg}} * G\beta_{\frac{\sigma\beta}{\lambda}}, \quad (10)$$

where $G\beta$ is a two-dimensional Gaussian function. Parameter β determines the size of the area over which summation takes place, values between 2 and 4 give good approximations of the spatial summation properties of grating cells. Orientations are combined by an amplitude operator

$$\mathcal{G}_{\text{all}\sigma,\lambda,\beta} = \sqrt{\sum_{i=0}^{N-1} (\mathcal{G}_{\sigma,\lambda,\theta_i,\beta})^2}, \quad (11)$$

where N denotes the number of orientations and $\theta_i = i\pi/N$, to yield the grating operator at a single scale.

4 Properties of grating cells

Von der Heydt et al. [5] describe responses to different synthetic grating patterns. In this section the properties of our grating cell operator are evaluated for different settings of parameters λ and γ , and results for different settings are compared with the measured data and the response properties of the model of Petkov and Kruizinga [3].

Von der Heydt et al. performed different tests to obtain the properties of periodic pattern selective cells in the monkey visual cortex. In the first test they revealed the *spatial frequency* and *orientation* tuning of the grating cells. From the second test they obtained the response properties to an increasing number of *cycles* of square-wave gratings. Their third test described the response

properties for *checkerboard* patterns by varying the check sizes. The fourth test tested the responses to so-called “Stresemann” patterns. These patterns are gratings where every other bar is *displaced* by a fraction of a cycle.

Finally they also tested the responses to contrast. The contrast profiles of the magno and parvo cells [1] show similarities with the profiles given by von der Heydt et al. [5]. In our experiments we will assume that contrast normalization on the input data took place by means of these magno and parvo cells, i.e. contrast normalization is applied to the input image. Hence, the test for contrast responses will be omitted in this study.

4.1 Responses to test patterns

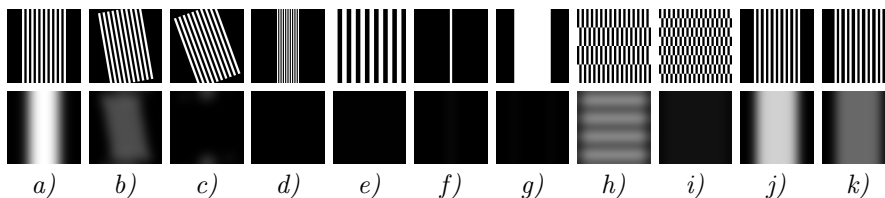


Figure 1: Responses to square gratings with different orientations and frequencies. Top row gives the stimulus and bottom row the responses of the modeled grating operator. *a)* Grating cells respond vigorously to grating patterns of preferred orientation and frequency. Responses decrease when the pattern differs from this pattern. *b)* and *c)* Responses strongly decrease if the gratings are rotated slightly (10 degrees) and completely vanish at 20 degrees. *d)* and *e)* Doubling or halving the frequency results in zero responses. *f)* and *g)* Grating cells hardly respond to single bars or edges. *h)* and *i)* Increasing the checks in a grating pattern results in a response decrease. *j)* and *k)* Stresemann patterns show similar behavior as in *h)* and *i)*: the stronger the deviation from *a)* the weaker its response. The used parameters are $\lambda = 1.00$, $\gamma = 0.25$, $\beta = 3.00$, $B_{\min} = 0.5$, and $B_{\max} = 2.5$.

Figure 1 illustrates that the modeled grating cell operator of (10) shows similar behavior compared to the measurements carried out by von der Heydt et al. [5]. Grating cells respond vigorously to grating patterns of preferred orientation and frequency, but any deviation from this pattern results in a decrease in response.

4.2 Orientation and frequency profiles

In this section the properties of grating cells will be modeled as accurate as possible by tuning parameters λ and γ to yield similar responses as measured by von der Heydt et al. [5] (denoted by “vdH ...” in the figures). In our model this orientation bandwidth corresponds to approximately $\lambda\gamma = 0.25$ (Fig. 2a).

Von der Heydt et al. found grating cells with both low and high frequency bandwidth. The response curves of these cells (Fig. 2b and c) are different. Most appropriate for the low frequencies is the model with parameters $\lambda = 1.00$ and $\gamma = 0.25$. Due to a problem that occurs for models with $\gamma > 0.4$, this choice is most suitable for high frequencies, also. For $\gamma > 0.4$ there are also responses

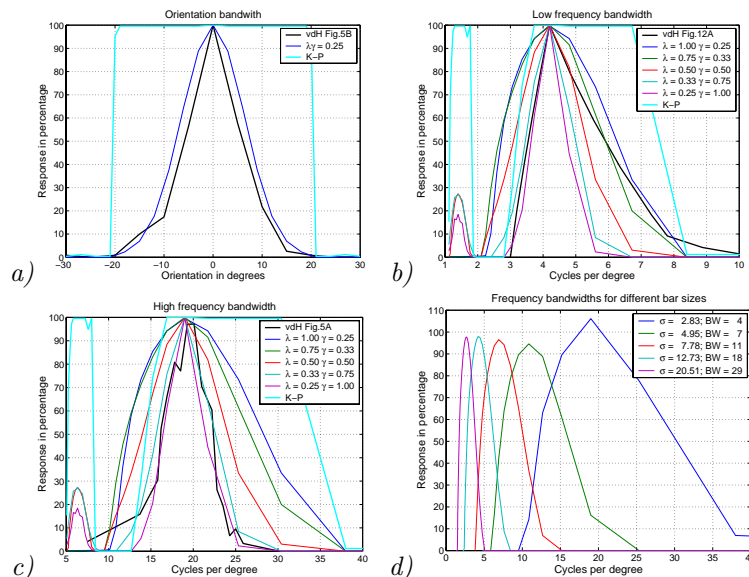


Figure 2: Measured and modeled response profiles of grating cells. *a)* Orientation, *b)* low frequency, and *c)* high frequency profiles. *d)* Frequency profiles for different preferred bar width sizes (BW = 4, 7, 11, 18, and 29 pixels). Cycles per degree have arbitrary units. Parameters used for *d)* are $\lambda = 1$ and $\gamma = 0.25$.

to frequencies that are about a factor 3 larger than the preferred frequency (Fig. 2b and c). The frequencies (in cycles per degree) are arbitrary units for the model, since the frequency is determined by the size of the image and the distance of the observer to the image.

Figure 2d illustrates the bandwidths for different preferred bar widths, respectively 4, 7, 11, 18, and 29 pixels. The figure illustrates that these 5 “scales” cover the full range of preferred frequencies (2.6 to 19 cycles per degree) found by von der Heydt et al. If a preferred bar width of 4 pixels is equivalent to 19 cycles per degree then 2.6 cycles per degree corresponds to a bar width of $4 \times 19 / 2.6 = 29.2$ pixels. The use of these five scales covers the full range well, since the lowest response, between two preferred frequencies, drops at most 25 percent from the maximum response.

The grating cell operator of Kruijzinga and Petkov, is available online (<http://www.cs.rug.nl/users/imaging/grcop.html>) and was used with a *bandwidth* of 1.0 and a *periodicity* that equals two times the preferred bar width. The response profile (in our figures denoted by “K-P”) of this grating operator shows globally two states: inactive or vigorously firing, which is caused by their normalization quantity q . The choice of $\lambda = 0.56$ gives strong responses in two intervals.

4.3 Profiles for different textures

Figure 3a illustrates that the measured results of the grating cells show increasing response with increasing number of bars. In the same figure only one modeled curve is shown, and although modeled grating cells with different pa-

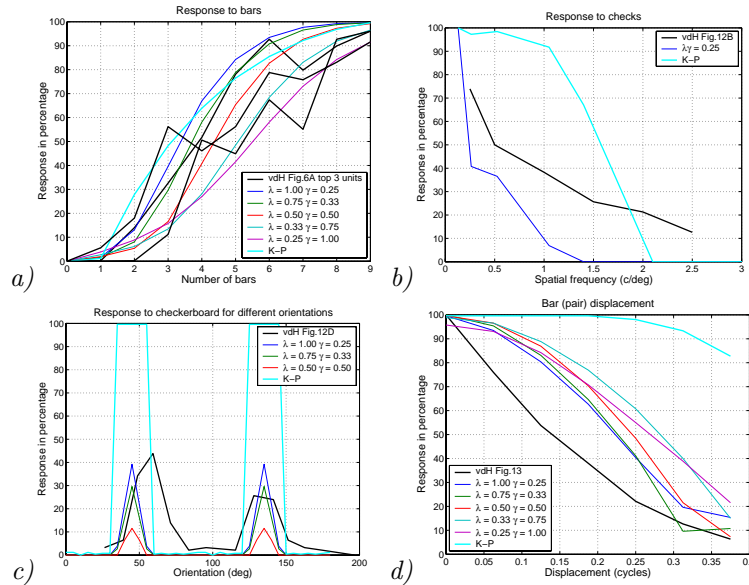


Figure 3: Measured and modeled properties of grating cells. *a)* Response profile for increasing number of bars. *b)* Response to checks. *c)* Sensitivity to different orientations of a checkerboard pattern. *d)* Responses to increasing shift of a pair of bars, the so-called Stresemann pattern.

rameters show different response curves they all are similar to the responses of the measured cells.

The modeled cells are not as robust to checks as the measured cells as illustrated in Figure 3b. On the contrary the modeled cells are slightly less sensitive to shifts of bars (Figure 3d). The responses to different orientations depends on the orientation bandwidth. If $\lambda\gamma = 0.25$ the orientation bandwidth is similar to that of a measured grating cell, but its response to a checkerboard pattern is low (about three times less) compared to that of the measured grating cells. On the other hand when $\lambda\gamma = 0.35$ the responses are comparable, but in this case the orientation bandwidth is wider than that of the measured cell.

5 Oriented repetitive alternating patterns

It is clear that the model for grating cells responds to grating patterns, but the question that rises is to what kind of real world patterns these cells respond. The latter is important will the operator be successfully applied in an artificial vision system. We used three (Brodatz, 111; ColumbiaUtrecht, 61; and VisTex, 166 images) freely available databases containing different textures.

In this application $N = 16$ orientations and $S = 5$ scales with $\sigma_0 = 4\lambda/\sqrt{2}$ and $\sigma_1 = 7\lambda/\sqrt{2}$ are used. The scales are combined with a maximum operator:

$$\mathcal{G}_{all,\lambda,\beta} = \max_{i=0}^{S-1} \mathcal{G}_{all,\sigma_i,\lambda,\beta} \quad (12)$$

and applied to the images in the databases.

The grating cell operator is very selective and responded in only five (samples 38, 46, 49, 51, and 57) images in the ColumbiaUtrecht database. The operator responded in 32 images of the Brodatz database. In the VisTex database the operator responded to three (buildings, fabric, and tile) out of 18 categories and within the categories it responded to about half of the images.

Based on these results, we conclude that grating cells respond well to man-made objects that have oriented alternating repetitive patterns.

6 Conclusions

We presented a new model for grating cells that has similar response profiles as monkey grating cells measured by von der Heydt et al. [5]. Unlike the previous models of grating cells (von der Heydt et al. [4] and Kruizinga-Petkov [3]) the new model accounts for proper spatial frequency tuning. The Kruizinga-Petkov model is an oriented texture operator, since it responds well to oriented texture. Although it is inspired by the work of von der Heydt et al. [5], it is not an accurate model of grating cells because the response profiles differ rather strongly from that of the measured grating cells.

We applied the new model to 338 real world images of textures from three databases. Based upon these results we conclude that grating cells respond to oriented texture, to oriented repetitive alternating patterns to be precise, but are insensitive to many other textures. In general, grating cells are not suitable for texture detection. The grating cell operator responds well if the complex cell responses perpendicular to the preferred orientation show similar strong responses. In such case it is impossible to detect or extract relevant edges in these areas by using complex cells. It therefore seems that grating cells could play a key role in separating form from texture by giving inhibitive feedback responses to the complex cells. A field which we want to explore in the near future.

References

- [1] E. Kaplan and R. M. Shapley. The primate retina contains two types of ganglion cells, with high and low contrast sensitivity. *Proc. Natl. Acad. Sci. U.S.A.*, 83:2755–2757, April 1986.
- [2] T. Lourens. *A Biologically Plausible Model for Corner-based Object Recognition from Color Images*. Shaker Publishing B.V., Maastricht, The Netherlands, March 1998.
- [3] N. Petkov and P. Kruizinga. Computational models of visual neurons specialised in the detection of periodic and aperiodic oriented visual stimuli: bar and grating cells. *Biological Cybernetics*, 76(2):83–96, 1997.
- [4] Rüdiger von der Heydt, Esther Peterhans, and Max R. Dürsteler. Grating cells in monkey visual cortex: Coding texture? Visual Cortex. In B. Blum, editor, *Channels in the visual nervous system: neurophysiology, psychophysics and models*, pages 53–73, London, 1991. Freund Publishing House Ltd.
- [5] Rüdiger von der Heydt, Esther Peterhans, and Max R. Dürsteler. Periodic-Pattern-selective Cells in Monkey Visual Cortex. *The Journal of Neuroscience*, 12(4):1416–1434, April 1992.